

$Q\bar{Q}$ modes in the Quark-Gluon Plasma

D. Cabrera^a and R. Rapp

Cyclotron Institute and Physics Department, Texas A&M University, College Station, TX 77843-3366, USA

Received: 8 November 2006

Published online: 15 March 2007 – © Società Italiana di Fisica / Springer-Verlag 2007

Abstract. We study the evolution of heavy quarkonium states with temperature in a Quark-Gluon Plasma (QGP) by evaluating an in-medium $Q\bar{Q}$ T -matrix within a reduced Bethe-Salpeter equation in S - and P -wave channels. The interaction kernel is extracted from finite-temperature QCD lattice calculations of the singlet free energy of a $Q\bar{Q}$ pair. Quarkonium bound states are found to gradually move across the $Q\bar{Q}$ threshold after which they rapidly dissolve in the hot system. We calculate Euclidean-time correlation functions and compare to results from lattice QCD. We also study finite-width effects in the heavy-quark propagators.

PACS. 25.75.Dw Particle and resonance production – 12.38.Gc Lattice QCD calculations – 24.85.+p Quarks, gluons, and QCD in nuclei and nuclear processes – 25.75.Nq Quark deconfinement, quark-gluon plasma production, and phase transitions

1 Introduction

Bound states of heavy (charm and bottom) quarks ($Q = b, c$) are valuable spectroscopic objects in Quantum Chromodynamics (QCD) [1]. When embedded into hot and/or dense matter a large class of medium modifications can be studied, including (Debye-) color-screening of the $Q\bar{Q}$ interaction, dissociation reactions induced by constituents of the medium, and the change in thresholds caused by mass (or width) modifications of open heavy-flavor states. Lattice QCD (lQCD) calculations have made substantial progress in characterizing in-medium quarkonium properties from first principles. In particular, it has been found that ground-state charmonia [2–4] and bottomonia [5] do not dissolve until significantly above the critical temperature, T_c , which has been supported in model calculations based on potentials extracted from lQCD, using either a Schrödinger equation for the bound-state problem [6–9], or a T -matrix approach which additionally accounts for scattering states [10]. More reliable comparisons to lQCD can be performed using (space-like) Euclidean-time correlation functions [11,12], which are readily evaluated in lQCD. The conversion of (time-like) model spectral functions requires a description not only of the bound-state part of the spectrum but also its continuum and threshold properties.

In the present work we evaluate Euclidean correlation functions for charmonium and bottomonium in a T -matrix approach. The basic input consists of in-medium $Q\bar{Q}$ potentials extracted from lQCD, inserted in a scattering

equation to calculate the in-medium $Q\bar{Q}$ T -matrix [10]. This incorporates bound and scattering states on an equal footing (based on the same interaction), and additionally enables a straightforward implementation of in-medium single-particle (quark) properties via self-energy insertions in the two-particle Green's function.

2 Scattering equation and bound states

The T -matrix equation for $Q\bar{Q}$ scattering in the center-of-mass frame and in partial-wave basis reads [10]

$$T_l(E; q', q) = V_l(q', q) - \frac{2}{\pi} \int_0^\infty dk k^2 V_l(q', k) G_{Q\bar{Q}}(E; k) T_l(E; k, q), \quad (1)$$

which follows from a standard 3-dimensional reduction of the Bethe-Salpeter equation [13]. $G_{Q\bar{Q}}(E; k)$ denotes the intermediate two-particle propagator including quark self-energies (Σ) and Pauli blocking. The T -matrix equation (1) is solved with the Haftel-Tabakin algorithm [14], in which the integral equation is solved by discretizing 3-momentum, $\sum_{k=1}^N \mathcal{F}(E)_{ik} T(E)_{kj} = V_{ij}$, and subsequent matrix inversion. The zeroes of $\det \mathcal{F}(E)$ for $E < E_{th}$ determine heavy quark-antiquark bound states.

The quark self-energy, Σ , encodes the interactions with (light) quarks and gluons from the heat bath [10]. In the present work we consider a fixed heavy-quark mass m_Q (i.e., $\text{Re } \Sigma = 0$) together with a small imaginary part, $\text{Im } \Sigma = -0.01 \text{ GeV}$, for numerical purposes. Effects of

^a e-mail: dcabrera@comp.tamu.edu

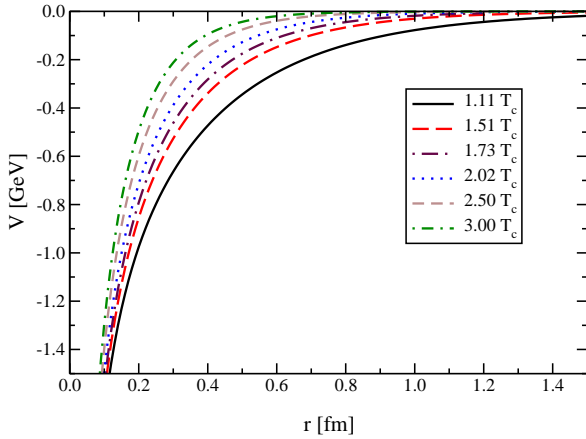


Fig. 1. $Q\bar{Q}$ potential for several temperatures above T_c based on the color-singlet internal energy.

temperature-dependent heavy-quark masses and widths are investigated in ref. [15].

The kernel of the scattering equation, V , can be estimated from the lQCD heavy-quark free energies, F_1 , even though there is still an ongoing discussion on how to properly do it. Here we identify the heavy-quark potential with the color-singlet internal energy, $U_1 = F_1 - T \frac{dF_1}{dT}$, which reproduces ground-state charmonium dissociation temperatures as found in lattice analysis of spectral functions [7–10]. In fig. 1 we show the $Q\bar{Q}$ potential, $V(r, T) = U_1(r, T) - U_1(r \rightarrow \infty, T)$, as obtained from a fit to the lQCD color-singlet free-energy data [16], previously employed in [10]. The potential evolves smoothly with temperature, decreasing both in magnitude and range. Different parameterizations of the lattice data imply sizable uncertainties in the potential through the thermal derivative of the free energy. These uncertainties are studied in ref. [15] by alternatively obtaining the heavy-quark potential from a direct fit to the lQCD internal energy data of ref. [17]. $V_i(q', q)$ follows from a Fourier transform and partial-wave expansion.

3 Quarkonium T-matrices in the QGP

We start the calculation of the in-medium $Q\bar{Q}$ T -matrices by fixing the heavy-quark masses so that the corresponding quarkonium ground states approximately agree with their vacuum masses for the lowest considered temperature ($T = 1.1T_c$), *i.e.*, $m_c = 1.7$ GeV and $m_b = 5.1$ GeV. Figure 2 summarizes the on-shell S -wave $c\bar{c}$ scattering amplitude as a function of the CM energy, for several temperatures. We do not include the hyperfine (spin-spin) interactions and therefore η_c (η_b) and J/ψ (Υ) states are degenerate. At the lowest temperature, we recover the charmonium ground state at $E \approx 3.10$ GeV, whereas the first-excited state (ψ') has just about melted. As the temperature increases, the $J/\psi(1S)$ gradually moves toward threshold and the T -matrix is appreciably reduced. The

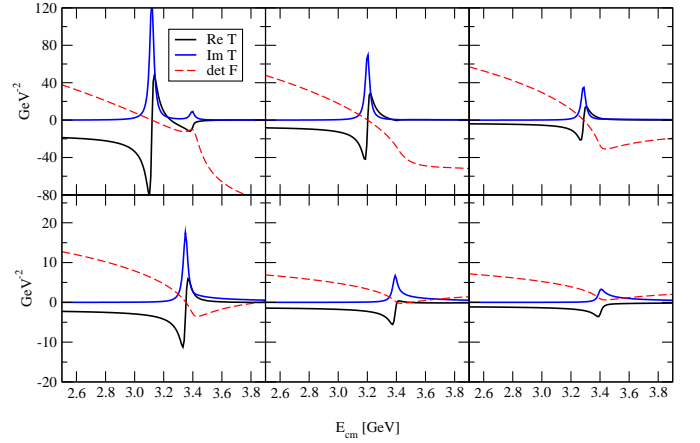


Fig. 2. T -matrix for S -wave $c\bar{c}$ scattering based on the potential in fig. 1. Also shown is $\det \mathcal{F}$ (dashed line, arbitrary units). From left to right (up-down) the temperatures are (1.1, 1.5, 2.0, 2.5, 3.0, 3.3) T_c .

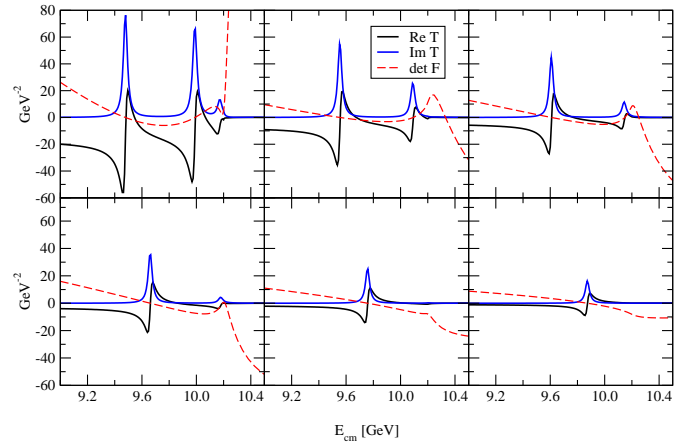


Fig. 3. Same as in fig. 2 but for S -wave $b\bar{b}$ scattering. From left to right and up to down the temperatures are (1.1, 1.5, 1.8, 2.1, 2.7, 3.5) T_c .

bound state survives up to $\sim 3T_c$, where it crosses the $c\bar{c}$ threshold and rapidly melts in the hot system.

The S -wave $b\bar{b}$ T -matrix exhibits two bound states at the lowest temperature ($E \approx 9.45, 9.95$ GeV for $\Upsilon(1S)$, η_b and $\Upsilon(2S)$, η'_b , respectively) and the remnant of a third one, which is (almost) melted in the medium, *cf.* fig. 3. The $\Upsilon(2S)$ moves across the $b\bar{b}$ threshold at $T \approx 2.1T_c$, whereas the $1S$ state survives in the QGP until much higher temperatures, beyond $T \approx 3.5T_c$.

We only find one P -wave bound state for the charm system at the lowest temperature, at $E \approx 3.4$ GeV, which we associate with the χ_c . The P -wave $b\bar{b}$ system exhibits two bound states at $1.1T_c$, with energies $E = 9.90, 10.15$ GeV, in good agreement with the nominal values for $\chi_b(1P)$ and $\chi_b(2P)$ in the vacuum. The latter moves beyond threshold at $T \approx 1.3T_c$, and the ($1P$) state at $T \approx 2.3T_c$. Masses and binding energies, ($E_B = E_{th} - M$), of the P -wave states are summarized in table 1 for several temperatures.

Table 1. Masses and binding energies (in GeV) for P -wave quarkonia as obtained from $\det \mathcal{F}(E) = 0$.

T/T_c	1.1	1.3	1.5	2	2.3
$M[\chi_c(1P)]$	3.4	–	–	–	–
$E_B[\chi_c(1P)]$	≈ 0	–	–	–	–
$M[\chi_b(1P)]$	9.90	9.98	10.04	10.14	10.20
$E_B[\chi_b(1P)]$	0.30	0.22	0.16	0.06	≈ 0
$M[\chi_b(2P)]$	10.15	10.20	–	–	–
$E_B[\chi_b(2P)]$	0.05	≈ 0	–	–	–

4 Spectral functions and Euclidean correlators

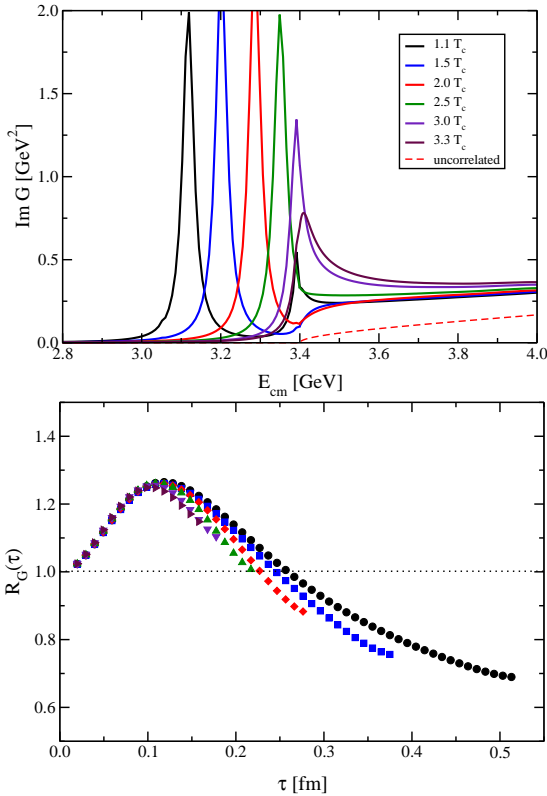
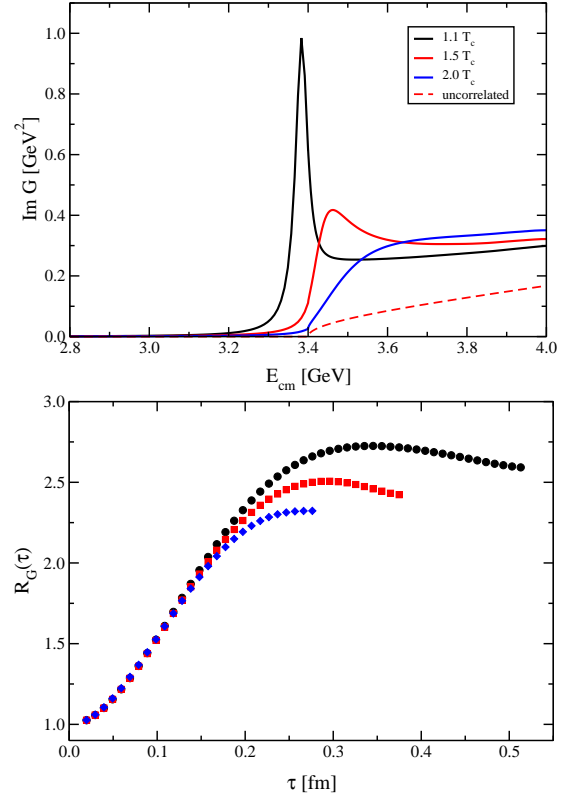
The Euclidean-time correlation function is defined as the thermal two-point mesonic correlation function in a mixed Euclidean-time momentum representation (here $\mathbf{p} = \mathbf{0}$),

$$G(\tau, T) = \int_0^\infty d\omega \sigma(\omega, T) \frac{\cosh[\omega(\tau - \beta/2)]}{\sinh(\omega\beta/2)}, \quad (2)$$

where σ is the spectral function obtained from closing external legs of the in-medium T -matrix, schematically as

$$G(E) = \int G_{\bar{Q}Q} + \int G_{\bar{Q}Q} T G_{\bar{Q}Q}, \quad \sigma(E) \propto \text{Im} G(E). \quad (3)$$

As expected, the S -wave charmonium spectral function (top panel of fig. 4) reflects the bound states of the

**Fig. 4.** Top: $c\bar{c}$ spectral function for S -wave scattering at several temperatures. Bottom: normalized correlation function at several temperatures.**Fig. 5.** Same as in fig. 4 for $c\bar{c}$ P -wave scattering.

T -matrix, but the (non-perturbative) $c\bar{c}$ rescattering also generates appreciable strength above threshold, where the remnant of the first-excited state ($\psi(2S)$) can be still inferred at $T = 1.1T_c$. The corresponding correlation function (bottom panel of fig. 4) is normalized to a “reconstructed” correlator represented by a zero-temperature spectral function consisting of a δ -function-like bound-state spectrum and perturbative continuum with onset at $E_{cont} = 4.5$ GeV [9]. The temperature evolution of the correlator is a combined result of a decrease in binding energy of the bound states and the contribution of the non-perturbative continuum. The sizable drop at large τ is in qualitative agreement with lQCD [3]. The latter exhibits somewhat less reduction, leaving room for the effects of a threshold reduction with temperature in our T -matrix.

The P -wave charmonium spectral function (fig. 5, top) exhibits one bound state (χ_c) just below the threshold, which rapidly melts into the continuum accompanied by a sizable threshold enhancement. The normalized correlator steeply rises in the low- τ regime, due to: i) non-perturbative rescattering and ii) a larger threshold in the “reconstructed” correlator. While this is qualitatively consistent with lQCD, the evolution with temperature is opposite, which could improve by a shift of strength to lower energies due to a decreasing heavy-quark mass with temperature. The bottomonium correlation functions follow a similar pattern as for the charmonium system.

It turns out that the τ -dependence of the (normalized) Euclidean correlators is rather sensitive to the “reconstructed” correlator used for normalization. However,

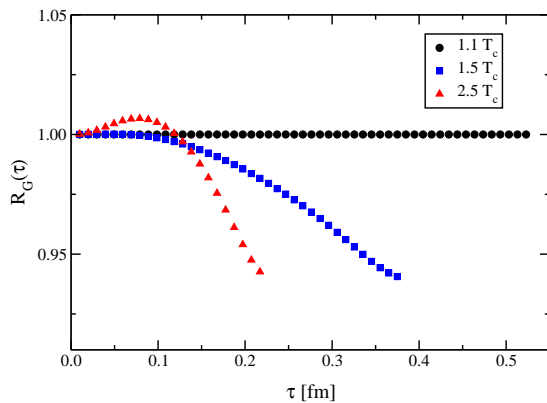


Fig. 6. S -wave charmonium correlators when replacing the “reconstructed” correlator (used for normalization) by the calculated result at $1.1 T_c$.

S -wave charmonium correlators from lQCD show rather little temperature dependence below $\sim 1.5 T_c$. Thus, to reduce ambiguities induced by the reconstructed correlator, we have normalized our correlators from the T -matrix to the result at $T = 1.1 T_c$ calculated in the same approach, cf. fig. 6. The τ -dependence is now substantially weaker than in the bottom panel of fig. 4 (limited to less than 10%), and the agreement with lQCD [3] is much improved.

We have also studied finite width effects for quarkonia by implementing c -quark widths of 0.05 GeV [18], inducing $\Gamma_\Psi \approx 0.1 \text{ GeV}$. The correlators show variations of the order of a few percent, indicating a small sensitivity to phenomenological (sizable) values of quarkonium widths.

We thank M. Mannarelli and F. Zantow for providing their (fits to) lattice QCD results, and M. Mannarelli and H. van Hees for useful discussions. This work is supported in part by Ministerio de Educación y Ciencia (Spain) via a postdoctoral fellowship and by a U.S. National Science Foundation CAREER Award under Grant No. PHY0449489.

References

1. N. Brambilla *et al.*, arXiv:hep-ph/0412158.
2. M. Asakawa, T. Hatsuda, Phys. Rev. Lett. **92**, 012001 (2004).
3. S. Datta, F. Karsch, P. Petreczky, I. Wetzorke, Phys. Rev. D **69**, 094507 (2004).
4. T. Umeda, K. Nomura, H. Matsufuru, Eur. Phys. J. C **39**, s1, 9 (2005).
5. K. Petrov, A. Jakovac, P. Petreczky, A. Velytsky, PoS (LAT2005) 153 (2006).
6. E.V. Shuryak, I. Zahed, Phys. Rev. C **70**, 021901 (2004).
7. C.Y. Wong, Phys. Rev. C **72**, 034906 (2005).
8. W.M. Alberico, A. Beraudo, A. De Pace, A. Molinari, Phys. Rev. D **72**, 114011 (2005).
9. A. Mocsy, P. Petreczky, Phys. Rev. D **73**, 074007 (2006).
10. M. Mannarelli, R. Rapp, Phys. Rev. C **72**, 064905 (2005).
11. R. Rapp, Eur. Phys. J. A **18**, 459 (2003).
12. A. Mocsy, P. Petreczky, Eur. Phys. J. C **43**, 77 (2005).
13. R. Blankenbecler, R. Sugar, Phys. Rev. **142**, 1051 (1966).
14. M.I. Haftel, F. Tabakin, Nucl. Phys. A **158**, 1 (1970).
15. D. Cabrera, R. Rapp, arXiv:hep-ph/0611134.
16. P. Petreczky, private communication (2004).
17. O. Kaczmarek, F. Zantow, arXiv:hep-lat/0506019.
18. H. van Hees, R. Rapp, Phys. Rev. C **71**, 034907 (2005).